

Innate lymphoid cells: NK and cytotoxic ILC3 subsets infiltrate metastatic breast cancer lymph nodes

Louise Rethacker^a, Maxime Boy^a, Valeria Bisio^a, France Roussin^b, Jordan Denizeau^c, Anne Vincent-Salomon^d, Edith Borcoman^{e,f}, Christine Sedlik^c, Eliane Piaggio^c, Antoine Toubert^{a,f,g}, Nicolas Dulphy^{a,f,g}, and Anne Caignard ^a

^aINSERM U1160, Institut de Recherche Saint-Louis, Hôpital Saint Louis, Paris, France; ^bService d'Anesthésie-Réanimation, AP-HP, Hôpital Saint-Louis, Paris, France; ^cINSERM U932, Département de Recherche Translationnelle, Institut Curie, Université de Recherche Paris Sciences & Lettres (PSL), Institut National de la Santé et de la Recherche Médicale (INSERM), Paris, France; ^dDiagnostic and Theranostic Medicine Division, Institut Curie, PSL Research University, Paris, France; ^eDepartment of Medical Oncology, Institut Curie, Paris, France; ^fUniversité Paris Diderot, Université de Paris, Paris, France; ^gAssistance Publique-Hôpitaux de Paris (AP-HP), Hôpital Saint-Louis, Laboratoire d'Immunologie et Histocompatibilité, Paris, France

ABSTRACT

Innate lymphoid cells (ILCs) – which include cytotoxic Natural Killer (NK) cells and helper-type ILC – are important regulators of tissue immune homeostasis, with possible roles in tumor surveillance. We analyzed ILC and their functionality in human lymph nodes (LN). In LN, NK cells and ILC3 were the prominent subpopulations. Among the ILC3s, we identified a CD56⁺/ILC3 subset with a phenotype close to ILC3 but also expressing cytotoxicity genes shared with NK. In tumor-draining LNs (TD-LNs) and tumor samples from breast cancer (BC) patients, NK cells were prominent, and proportions of ILC3 subsets were low. In tumors and TD-LN, NK cells display reduced levels of NCR (Natural cytotoxicity receptors), despite high transcript levels and included a small subset CD127⁻ CD56⁻ NK cells with reduced function. Activated by cytokines CD56⁺/ILC3 cells from donor and patients LN acquired cytotoxic capacity and produced IFN γ . In TD-LN, all cytokine activated ILC populations produced TNF α in response to BC cell line. Analyses of cytotoxic and helper ILC indicate a switch toward NK cells in TD-LN. The local tumor microenvironment inhibited NK cell functions through downregulation of NCR, but cytokine stimulation restored their functionality.

ARTICLE HISTORY

Received 15 November 2021
Revised 20 March 2022
Accepted 20 March 2022

KEYWORDS

Innate lymphoid cells; natural killer cells; tumor draining lymph nodes; breast cancers

Introduction

Innate lymphoid cells (ILC) are important contributors to the immune homeostasis of tissues. They include NK cells or cytotoxic ILC1, endowed with cytotoxic functions toward transformed cells, and helper-type ILC (h-ILC) characterized by the expression of CD127 (IL-7 R α). While NK and h-ILC development is initiated in the bone marrow, these effectors mature and terminally differentiate in secondary lymphoid tissue (SLT). For NK cells, LNs represent important sites of maturation and differentiation and several NK precursors have been described. Following the recent identification of h-ILCs, NK development in LNs requires further investigation as certain intermediates previously defined as NK cells may in fact correspond to h-ILCs.

ILCs are classed in three groups based on helper T cell nomenclature.¹ Among h-ILCs, ILC1 are CD117⁻CRTH2⁻, produce IFN γ and TNF α , and express the transcription factor (TF) T-bet; ILC2 are CD117⁺CRTH2⁺, produce IL-5 and IL-13, and express GATA3 and RORA; and ILC3 are CD117⁺ CRTH2⁻, produce IL-17 and IL-22 in response to IL-23 and IL-1 β , and express ROR γ t. ILC3 can express the natural cytotoxicity receptors (NCR) NKp44, NKp46, and NKp30. CD56⁺CD127⁻ NK cells – cytotoxic ILC1 – express T-bet and Eomes and produce IFN γ , TNF α , the cytotoxic

molecule perforin, and granzymes. In contrast to NK cells, h-ILCs are rare in the blood but abundant in tissues, where the environment determines their heterogeneity.² Indeed, signals received from their environment produce an interesting feature in ILC by stimulating their capacity to trans-differentiate. For example, cytokines, such as IL-12/IL-15, IL-12/IL-2 favor ILC1/NK plasticity, whereas IL-23/IL-1b/IL-7 favor ILC3/ILC1 plasticity.^{3–5} To identify all ILC subsets, specific gating and labeling strategies must be applied⁶ distinct from those used for NK cells. However, distinguishing between NK and ILC1 remains complex to do on a phenotypic basis, particularly in a tumor microenvironment.^{7–9} For example, stage 3 NK cells have been reported in human SLT as CD34⁻CD117⁺CD127⁺CD56⁺CD94⁻, producing IL-22 and expressing the transcription factor AHR.^{10,11} Some studies affirmed that this population includes ILC3,¹² indicating that stage 3 NK cells and ILC3 have phenotypic similarities.

For some solid tumors, the LN is the primary site of tumor spread. Moreover, in Breast cancer (BC) patients, the presence of LN metastases correlates with decreased 5-year survival.¹³ The LN is an important site for the immune response and the presence of metastases in this organ leads to a change in the microenvironment that can alter the immune response. Given

the role of tumor-draining LN (TD-LN) in the dissemination of cancer cells and emergence of distant metastases, we investigated the ILC populations in healthy-donor LN (HD-LN) and compared them to those from TD-LN and tumors from BC patients.

LNs contain a majority of CD56^{bright} CD16⁻ NK cells with minor proportions of CD16⁺ NK cells.¹⁴ Few reports have described the presence of h-ILC in human LN. In mice, ILC3 is the major population in LNs.¹⁵

NK cells infiltrate various healthy tissues and are attracted to inflamed and tumor tissues.^{16,17} NK cell activation depends on a fine balance between activating and inhibitory signals that determines whether the target cell will trigger the NK cell killing program. Natural Cytotoxicity Receptors (NCRs) NKp46 and NKp30, expressed by resting NK cells, and NKp44, induced by cytokines,^{18,19} trigger the lysis of various tumor cells, including BC cells.²⁰ ILC3 can express NCRs, and engagement of NKp44 has been shown to activate the production of IL-22 and GM-CSF.^{21,22} The Natural Killer Group 2 (NKG2D) receptor binds MHC class I polypeptide-related sequence (MIC)-A/B molecules and UL16-binding proteins 1–6 (ULBP1–6), which are induced on stressed cells.²³ The adhesion DNAX accessory molecule-1 (DNAM-1) binds to nectin and nectin-like proteins. NKG2D and DNAM-1 also promote tumor cell elimination.²⁴ NK cell activation is controlled by HLA class I-specific inhibitory NK receptors. The CD94/NKG2A heterodimer binds to HLA-E molecules, and the killer immunoglobulin-like receptors (KIRs), bind to specific HLA class I alleles.^{19,25} The inhibitory members of DNAM-1 family receptors – CD96 and TIGIT – compete with DNAM-1 for ligand binding, and limit NK cell function by direct inhibition.^{26,27} In both experimental tumor models and human tumors, NK cells can control metastasis formation.^{28–31} However, tumor cells may escape NK cell immunosurveillance through several mechanisms, and tumor-infiltrating NK cells often display phenotypic alterations.^{32–35} NK immunosuppression must be targeted to restore functionality and promote the immune control of metastatic BC.³⁶ How h-ILC are involved in tumor surveillance is still poorly understood, especially in humans.³⁷ These cells have been shown to exhibit both anti- and pro-tumor responses in a number of tumor types.⁹ Thus, ILCs represent interesting focuses for immunotherapy when treating solid tumors, and can be targeted by immune checkpoint blockers (ICBs). For example, ILC2 express CTLA-4 and PD-1 in inflammatory breast cancer, and in gastrointestinal cancer both ILC2 and ILC3 express PD-1.³⁷

Given this context, in this study, we first characterized ILC subsets from HD-LN. We then analyzed the ILC in TD-LN and in tumor from BC patients to allow a better understanding of the tumor impact on ILC subsets.

Materials and methods

Samples and patients

TD-LNs and tumors were collected from 28 patients, with luminal BC having undergone standard-of-care surgical resection at the Institut Curie Hospital (Paris, France).

Tissue samples were taken from surgical residues available after histopathologic analyses and not required for diagnosis. Our human experimental procedures follow the Declaration of Helsinki guidelines and were approved by the Institutional Review Board and Ethics committee of the Institut Curie Hospital group (CRI-0804-2015). Patients did not receive any prior treatments other than surgery. Supplementary Table 1 summarizes the mutational status of the patients.

Organ donor-derived mesenteric LNs (n = 28) were obtained from the Intensive Care Unit at Saint Louis Hospital (Paris, France) following ethical procedures and analyzed as non-cancer controls (healthy donor, HD-LNs). HD-LN included 15 women and 13 men (median age of 61 years old). Tissues were mechanically dissociated and incubated one hour at 37°C in collagenase IV, hyaluronidase, and DNase I. Dissociated tissue were stored in liquid nitrogen.

Flow cytometry staining and cell sorting

Frozen cells were thawed, washed twice, and counted; their viability was assessed by trypan blue exclusion before labeling. Samples were stained with Flexible Viability Dye eFluor 506 (eBioscience) for 30 min before staining with surface antibodies (Table S2) in brilliant Stained Buffer (BD) at 4°C for 30 min. For intracellular staining, cells were fixed and permeabilized for 3 min in FoxP3 buffer (eBioscience) before staining with anti-Eomes, anti-T-bet, anti-ROR γ t, anti-perforin, and anti-granzyme B (BD). Cells were fixed and data were acquired on an LSRFortessa (BD).

For cell sorting, samples were depleted of lineage positive (Lin⁺) cells using the EasySep FITC positive selection Kit II (Stemcell). The lineage mix included antibodies against CD3, CD4, CD5, TCR $\alpha\beta$, TCR $\gamma\delta$ (T cells), CD33, CD14 (myeloid cells), CD19 (B cells) and CD235a (erythrocytes). 100 cells per subset were sorted according to the gating strategy shown in Figures 2(a) and 5(a).

viSNE and CITRUS analysis

Lin⁻CD7⁺ cells were pre-gated with FlowJo10 (BD). Samples were analyzed using viSNE in Cytobank, first individually and then after concatenating files. The viSNE map was clustered using FlowSOM (Cytobank).³⁸ The CITRUS algorithm (Cytobank) was used to compare the abundances of ILC subsets and marker expression levels between TD-LN and tumor samples. CITRUS was used to build a hierarchical clustering tree based on similarities in levels of marker expression. The minimum cluster size for events among the total data used was 1%, and 120 events were sampled per file. The analysis was based upon abundance of events using Significance Analysis of Microarrays (SAM), with a false discovery rate of 0.01.

CD107a degranulation and cytokine release assays

Cells from LN cell suspensions were stimulated overnight in medium containing IL-2 (10 ng/mL) and IL-12 (5 ng/mL) (Miltenyi Biotec) and then co-cultured for 5 h with K562 or

MCF7 cells (breast cancer cell line) at a 1:1 effector:target ratio. Co-cultures were performed in U-bottom plates in the presence of Golgi Stop (BD Biosciences), Brefeldin A (BD), and CD107-FITC antibody (Table S2). Cells were then stained with Flexible Viability Dye eFluor 506 (eBioscience) for 30 min before labeling with surface antibodies (Table S2). To stain intracellular IFN γ and TNF α , cells were fixed and permeabilized for 30 min in FoxP3 buffer (eBioscience) before incubating with anti-IFN γ -APC (BD) and anti-TNF α -PECy7 in perm buffer for 30 min.

Multiplex RT-qPCR

Cells were directly sorted into the reaction mix of the SuperScript III One-Step RT-PCR System containing Platinum Taq DNA Polymerase (Invitrogen). In the first step, RNA was reverse-transcribed to cDNA, and cDNA was pre-amplified for 19 cycles using target gene TaqMan primer pool (Supplementary Table 3), according to the manufacturer's instructions. After pre-amplification, the reaction mixtures were loaded onto a Fluidigm microfluidic chip using the Juno system (Fluidigm), and the chip was used with the BioMark real-time PCR reader (Fluidigm). All expression data were normalized relative to *GAPDH* expression, and relative quantification levels were calculated. Primers were exons spans probes designed and validated by the provider (Thermo Fisher), thus avoiding gDNA contamination.

Statistics

Statistical tests were performed using Prism version 8 (GraphPad Software Inc). A non-parametric Wilcoxon matched-pairs signed-rank test was used to compare mRNA expression levels between different ILC subsets. The Mann-Whitney test was used to compare mRNA levels between healthy donors and BC patients. Principal component analysis (PCA) to visualize and organize the multivariate data from donors was performed in R. Heatmaps were produced and hierarchical clustering was done using <http://www.heatmap.per.ca/>.

Results

Phenotype of innate lymphoid cells in lymph nodes from HD

The first step in our study was to characterize ILC subsets in HD-LN. ILCs were gated as lineage-marker-negative cells expressing CD7 (lin⁻CD7⁺ cells), and represented 1–2% of live cells contained in LNs. To distinguish between and determine the relative proportions of the different ILC populations, we performed a viSNE analysis and FlowSOM clustering on pooled data from 13 HD-LN (Figure 1(a)). The analysis was based on expression levels for the backbone markers: CD127, CD117, CRTH2, CD56, and CD16. These markers were previously described^{1,39} to distinguish NK cells (cytotoxic ILC1) from helper-type (h-ILC) subsets (ILC1, ILC2, ILC3) on the viSNE map

(Figure 1(a,b)). This analysis revealed HD-LNs to contain four main ILC populations: NK cells, defined as CD56^{bright}CD127⁻ which included CD16⁺ (10%) and CD16⁻ (39%) sub-populations, and two populations of h-ILCs based on the expression of CD56, the CD127⁺CD56⁻ and a prominent CD127⁺CD56⁺ cell subset (40%) population (Figure 1(a), right panel). The CD127⁺CD56⁻ h-ILC correspond to three subsets: CD127⁺CD117⁺CD56⁻ ILC3 cells (12% of total lin⁻CD7⁺ cells), a discrete subset of CD117⁻CRTH2⁻ ILC1 (< 5%) and few CRTH2⁺CD117⁺ ILC2 (~0.3%). The CD127⁺CD56⁺ cell subset was defined by the expression of CD127, CD56, and CD117, and was considered as an CD56⁺/ILC3 population (Figure 1(b)).

As shown on the viSNE map, LN-NK cells expressed the following NCR: NKp46, NKp30, and NKp44 (Figure 1(b)). NK cells displayed higher NKp46 and NKp30 expression than CD56⁺/ILC3 and ILC3, while NKp44 was higher on h-ILC than on NK cells (Fig. S1). Although percentages of CD56⁺/ILC3 cells expressing NKp44 and NK46 largely varied among samples, but it confirmed NCR expression by these ILC subset.⁴⁰ NKG2D expression appeared spread among samples with a comparable expression on ILC subsets (Figure 1(b) and Fig. S1).

CD94 was expressed by a high proportion of NK cells (93%), absent from ILC3 and detected on <10% of CD56⁺/ILC3. NKG2A was present on a higher fraction of NK cells (40%) than on CD56⁺/ILC3 (25%) and detected on 10–15% of ILC3. TIGIT was expressed by moderate fractions (30–40%) of NK cells and absent from h-ILC (Figure 1(c)). All three cell subsets – NK cells, ILC3s, and CD56⁺/ILC3s – expressed CD161 and DNAM-1. Among the NK cells, 52% of NK cells co-expressed CD69 and CXCR6. CXCR6 was faintly expressed by other ILC populations (Figure 1(d)). The residency marker CD69 was strongly expressed by most h-ILC cells (Figure 1(e)). Within the CD56⁺/ILC3s, a small subset co-expressing CD103 alongside CD69 and NKp44 was identified (Figure 1(e)). This subset is close to the intraepithelial (IE) ILC1s previously described in mucosal and in non-mucosal tissues.^{41,42}

In conclusion, HD-LNs contained 3 main ILC subsets, NK cells, ILC3s, and a major CD56⁺/ILC3 subset.

Molecular signature of ILC in healthy-donor LNs

To further analyze the HD-LN ILC, the three major ILC subsets were sorted from 4 or 6 HD-LN and their transcriptomic profiles were determined by multiplex qPCR.³⁹ ILC3s and CD56⁺/ILC3s displayed close molecular profiles considering h-ILC population definition markers (Fig S2A), NK cell-specific genes (Fig. S2B) and genes common to h-ILC and cytotoxic ILCs (Fig S2C). Data were submitted to PCA to determine the differences between NK cells, ILC3, and CD56⁺/ILC3s (Figure 2(a,b)). As expected, this analysis indicated that CD56⁺/ILC3s were more closely related to ILC3 than to NK cells. The mRNA transcript levels for the markers defining the ILC subsets confirmed their phenotypic classification by viSNE (Figure 2(c)). High levels of transcripts were detected for *IL7R* (CD127) and *KIT* (CD117) in both CD56⁺/ILC3s cells and ILC3. Interestingly, among the variables contributing to PC1 and PC2, compared to ILC3s, CD56⁺/ILC3s

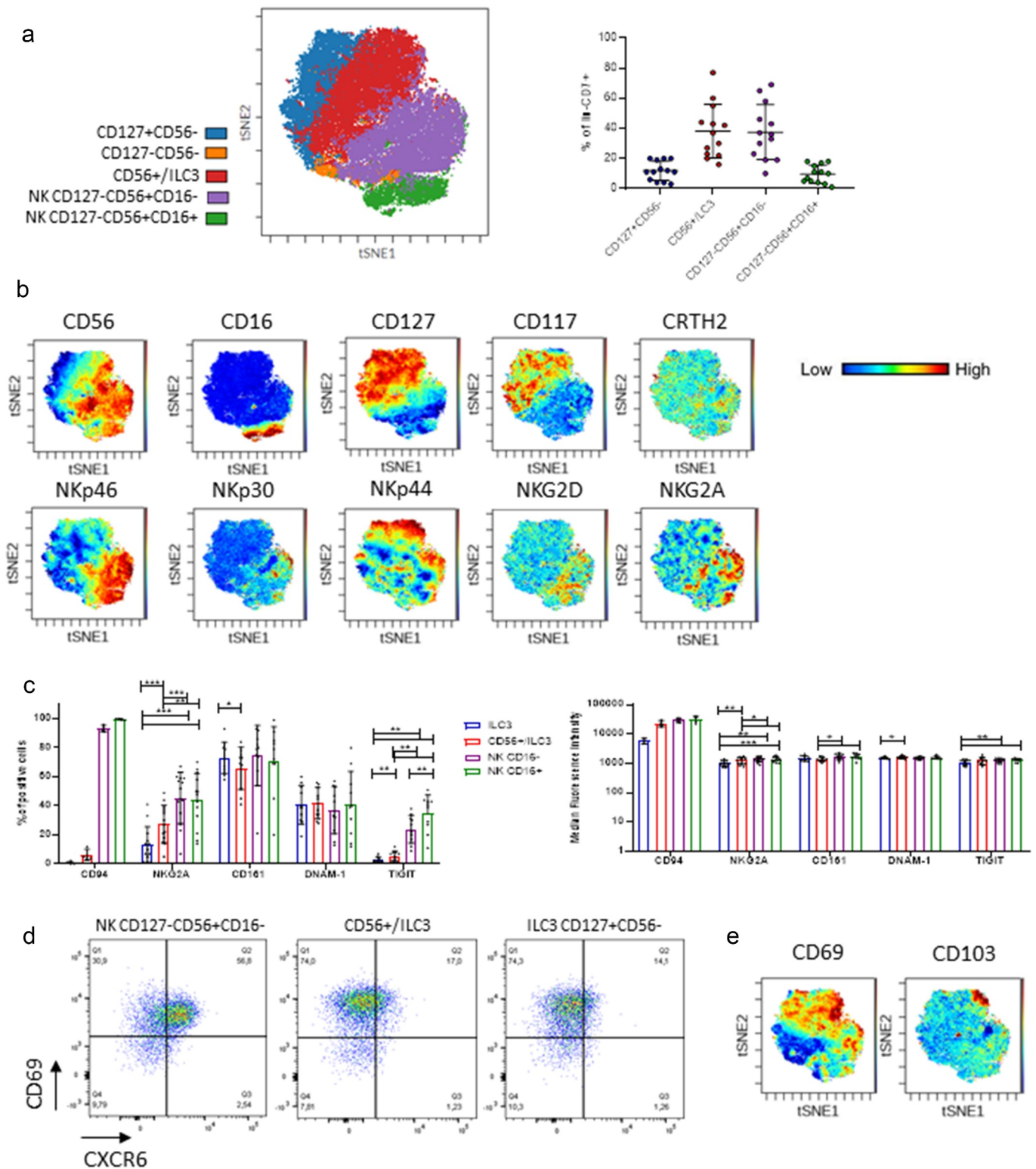


Figure 1. Innate lymphoid cells in lymph nodes from healthy donors. viSNE map of $\text{lin}^- \text{CD7}^+$ cells from HD-LNs (concatenated data), showing the FlowSOM clustering of ILCs, each color represents a subset. Percentages of ILC populations in HD-LN ($n = 13$) (a). viSNE map showing expression levels for specific markers using a color scale, from blue (low) to red (high) (b). Statistical analysis of CD94, NKG2A, CD161, DNAM-1 and TIGIT receptors expression by ILC subsets from 13 HD-LN (4 HD-LN for CD94) (c). Representative dot plots of CD69 and CXCR6 co-expression by HD-LN ILCs (d). viSNE map with CD69 and CD103 expression in 13 HD-LN ILC (e).

expressed higher levels of transcription factors *EOMES* and *TBX21* (coding for T-bet), both of which are implicated in NK cell differentiation (Figure 2(d)). At the protein level, CD56+/ILC3s expressed low levels of Eomes and did not express T-bet; in contrast, NK cells did faintly express T-bet (Fig. S3).

CD56+/ILC3s also expressed low levels of *RORC* – the TF required for ILC3 differentiation – at both the transcriptional and protein levels. ILC3s and CD56+/ILC3s expressed similar levels of *AHR*, which was expressed at lower levels by NK cells.

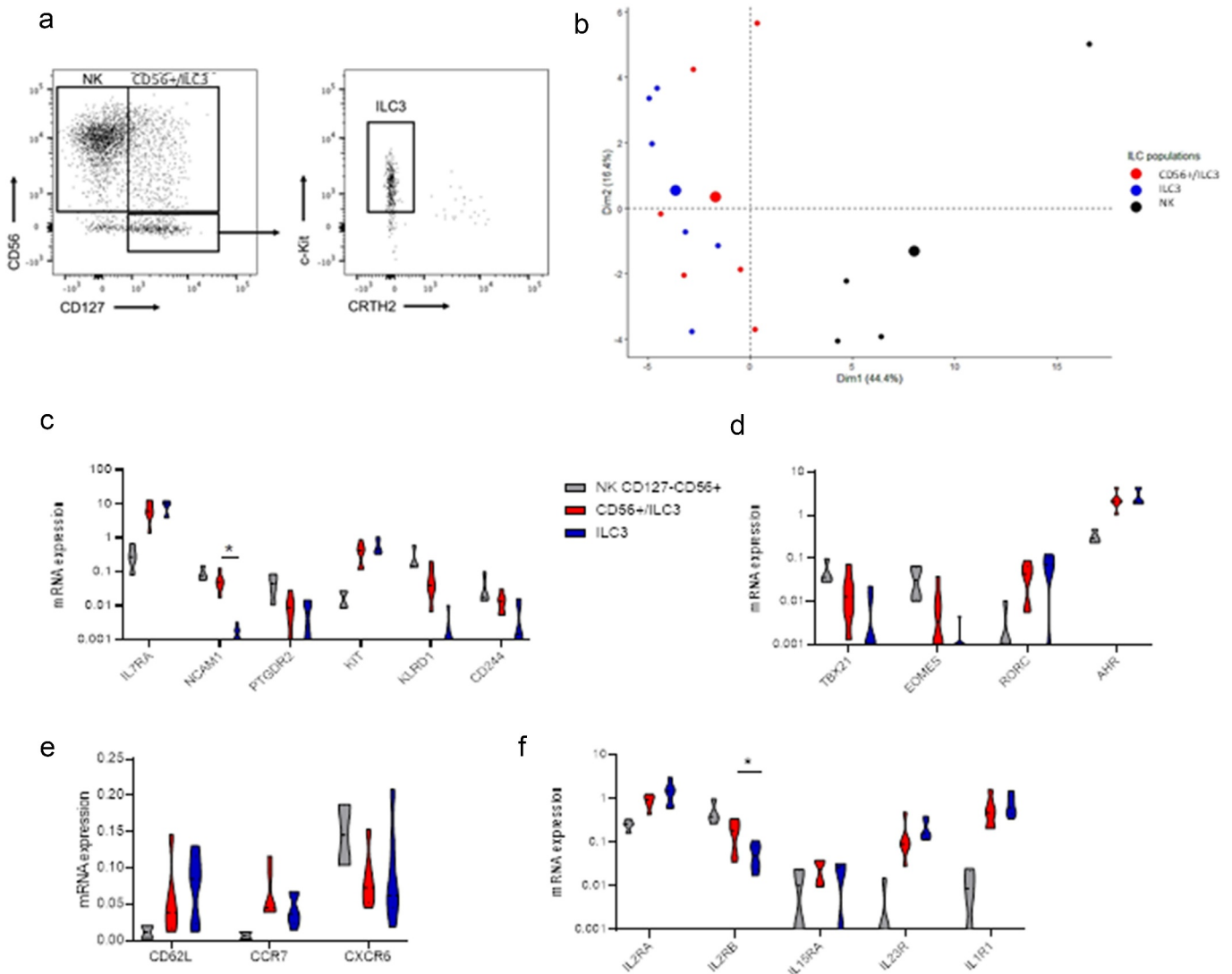


Figure 2. Transcriptional signature of ILC subsets in LN from healthy donors. Gating strategy for cell sorting of ILC subsets (a). Principal component analysis (PCA) of ILC subsets (n = 4/6) (b). mRNA expression of the principal variables contributing to PC1 and PC2 including ILC subset definition markers, transcription factors, as well as chemokine and cytokine receptors. A Wilcoxon's matched-pairs test was used to compare expression levels between two populations (* p < .05)(c-f).

In NK cells, transcript levels for chemokine receptors CD62L and CCR7 were low, whereas CXCR6 transcripts were high. In ILC3s and CD56⁺/ILC3s, CD62L and CCR7 transcripts were abundant, whereas CXCR6 transcripts were low (Figure 2(e)).

Finally, CD56⁺/ILC3s expressed the genes *IL2RA*, *IL23R*, and *IL1R1*, and may respond to IL23 and IL-1 as ILC3 (Figure 2(f)). They also expressed *IL2RB* and *IL15RA*, which are mostly expressed by NK cells.

Functional properties of ILC in healthy-donor LNs

CD56⁺/ILC3s expressed genes involved in cytotoxic functions, suggesting that they might behave like NK cells (Figure 3(a)). For example, they expressed transcripts of *PRF1* and *GZM* genes (*A*, *B*, *K*, and *H*), although at lower levels than NK cells. CD56⁺/ILC3s also expressed the Th1 type cytokines *IFNG* and *TNFA*, along with cytokines produced by ILC3: *CSF2* (coding for GM-CSF), and *IL22* in certain samples. At steady state, the protein levels for perforin and granzyme B were low in CD56⁺/ILC3 cells compared to NK cells (Figure 3(b)). Expression of these

two cytotoxicity markers was induced in CD56⁺/ILC3 cells after overnight activation with IL-2 and IL-12 (Figure 3(b)). We also assessed the cells' capacity to degranulate and to produce IFN γ following IL-2+ IL-12 activation and stimulation with K562 and MCF7 (Figure 3(c)). NK cells and CD56⁺/ILC3s degranulated and produced IFN γ upon stimulation with K562, whereas ILC3s did not (Figure 3(c)). In response to stimulation with the ER⁺ HLA-I⁺ BC cell line MCF7, the levels of degranulation and IFN γ production were low in NK cells and CD56⁺/ILC3s. No differences in the phenotype distribution and function of HD-LN ILC subsets were observed considering the gender issue.

ILC infiltrating metastatic LN and primary BC tumors

To examine how the tumor microenvironment affects LN-ILC populations, we then analyzed the ILC that infiltrated metastatic TD-LN from BC patients. The ILC phenotypes from metastatic TD-LN were compared to the ILC phenotypes infiltrating primary tumors from BC patients (luminal type, ER+, or ER/PR+). In tumors and axillary TD-LNs, the percentages of

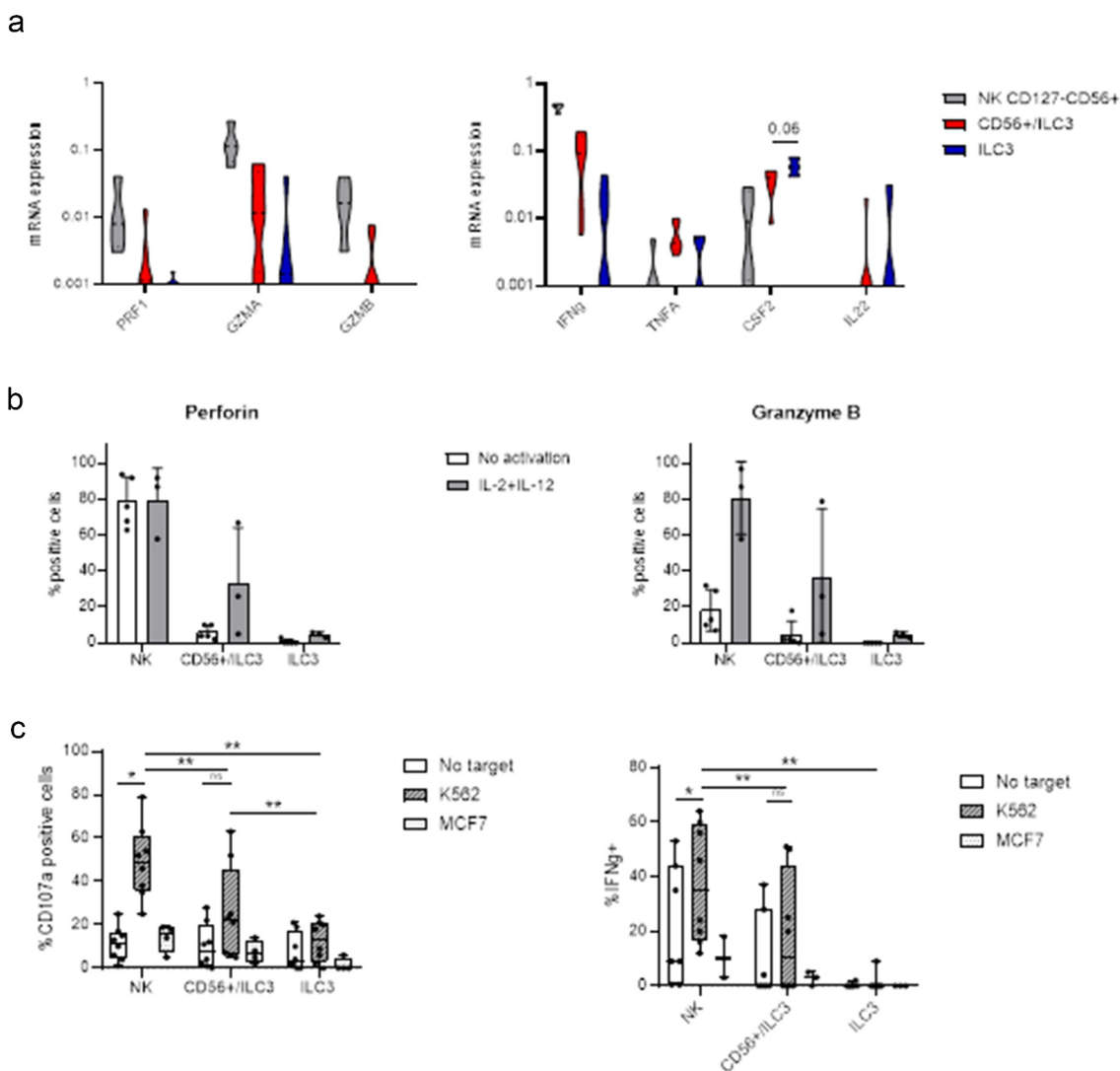


Figure 3. Functional capacities and plasticity of ILC in HD-LN. mRNA expression of cytotoxic molecules and cytokines in NK cells, CD56⁺/ILC3 ILC, and ILC3 (n = 4/6) (a). Percentages of cells expressing perforin and granzyme B before and after activation by IL-2 and IL-12 (n = 1/4) (b). ILC activated overnight with IL-2 and IL-12 were stimulated with K562 and MCF7 for 6 h. Then, percentages of degranulating cells (CD107a-positive cells), and expression of intracellular IFN γ in ILC subsets were determined by flow cytometry (n = 3); 'no target' corresponds to spontaneous degranulation (c). A Wilcoxon's matched-pairs test was used to compare expression levels between two populations (* p < .05)(c-f).

ILCs varied extensively across samples. The ILCs represented between 3% and 18% (mean 6%) of tumor infiltrating lin⁻CD7⁻ cells and while they represented between 0.5% and 6% (mean 2%) of lin⁻CD7⁺ cells from TD-LN (data not shown).

From viSNE analysis of TD-LN (n = 11) and tumor samples (n = 9), five ILC populations were identified (Figure 4(a)). In the two compartments, NK cell subsets were overrepresented among ILC (Figure 4(a), right). There was an abundant subset of CD127⁻CD56⁺CD16⁻ NK cells (60% and 78% in TD-LN and Tumor, respectively) and a small subset of mature differentiated CD56⁺CD16⁺ NK cells (3% in Tumor and 6% in TD-LN). In tumors, the proportion of h-ILC was low, with each ILC3 and CD56⁺/ILC3 subset representing less than 5%. In contrast, among total ILC in TD-LN, ILC3 represented 7%, and CD56⁺/ILC3s represented 16%. In addition, an expanded CD127⁻CD56⁻ ILC subset was identified in both sample types, corresponding to 4% of ILC in tumor and 2% in TD-LN (Figure 4(a), right). CD56⁻CD127⁻ cells were CD117⁻, NCR⁻, CD16⁻ in both compartments.

CITRUS analysis compared the frequencies of the ILC subsets defined by the backbone markers in LN and tumors, and detailed their phenotypic profiles (Figure 4(b-e)). Tumor-infiltrating NK cells contained two prominent CD56⁺NCR⁻CD69⁺CD103⁺ and CD103⁻ NK subsets, whereas ILC3 and CD56⁺/ILC3s were more prevalent in TD-LN (Figure 4(b,c)). CD56⁺CD16⁻ NK cells infiltrating TD-LN were characterized as NCR⁺ (NKp46, NKp30) and NKG2A^{low}, whereas tumor-infiltrating CD56⁺CD16⁻ NK cells were NCR⁻, NKG2A⁺. CD56⁺CD16⁺ NK cells were NKp46⁻ in LN and NCR⁺ in tumors. CD56⁺/ILC3s from TD-LN and tumors expressed low levels of NKp44 and NKp30.

NCR^{low}CD69⁺ NK cells expanded in the tumor were found in metastatic TD-LN exhibiting reduced CD69 expression suggesting their capacity to migrate to the TD-LN and supplant h-ILC. This marker was also expressed by ILC3 and CD56⁺/ILC3s in both compartments. Finally, ILC3 from the two compartments exhibited a similar phenotype.

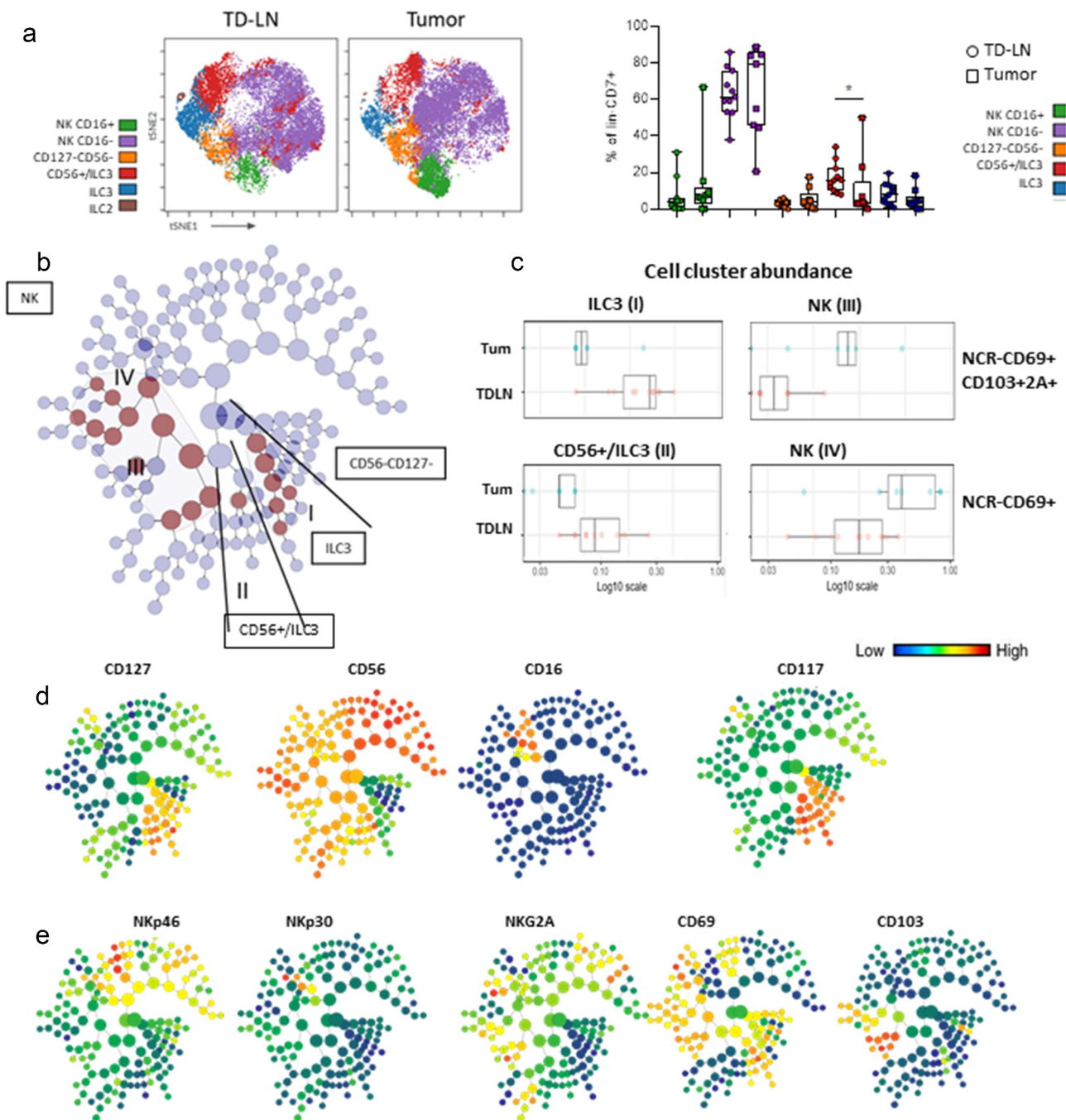


Figure 4. ILC infiltrating TD-LN and tumor. viSNE map for $\text{lin}^- \text{CD7}^+$ cells showing the FlowSOM clustering for ILC from TD-LN ($n = 9$) and tumors ($n = 11$). Percentages of ILC subsets present in TD-LN and tumor (a). Hierarchical clustering produced by CITRUS analysis comparing TD-LN ($n = 11$) and BC tumors ($n = 9$), identified in brown/dark red, showing four clusters for which cell abundances were significantly different between the two conditions (b). CITRUS map showing the expression levels for the backbone markers CD127, CD56, CD117, and CD16 using a color scale, from blue (low) to red (high) (c). Cell abundance in the different clusters (d). CITRUS map showing expression levels for NKp46, CD69, and CD103 (e).

Molecular profile of ILCs infiltrating metastatic LNs

To further study the five ILC subsets infiltrating TD-LNs, a transcriptomic analysis was performed on purified cells from metastatic TD-LNs ($n = 5$). The ILC subsets were the following: $\text{CD56}^+ \text{CD16}^-$, $\text{CD56}^+ \text{CD16}^+$ NK cells, unconventional $\text{CD56}^- \text{CD127}^-$ cells, ILC3, and $\text{CD56}^+ / \text{ILC3}$ s (Figure 5(a)). Transcript levels for backbone markers of ILC subtypes confirmed the phenotypic analyses. According to PCA, $\text{CD56}^+ / \text{ILC3}$ s segregated close to ILC3, and $\text{CD127}^- \text{CD56}^-$ were intermediate between

conventional ILC3 and NK cells (Figure 5(b)). NK and ILC3 subsets were segregated based on *NCAM1* (CD56), *GRZMA*, and *NKG2D* overexpression in NK cells; whereas ILC3s expressed high levels of *AHR*, *IL1R1*, *IL2RA*, and *CD69* (Figure 5(c)). The $\text{CD127}^- \text{CD56}^-$ NK subset expressed low levels of *IL7RA* (CD127) like NK cells, but low *NCAM1* (CD56) transcripts like ILC3s, and high levels of *KIT* (CD117) close to the levels expressed by h-ILCs (Figure 5(d)). With regard to TF genes, $\text{CD127}^- \text{CD56}^-$ cells expressed levels of *RORC* close to those detected in

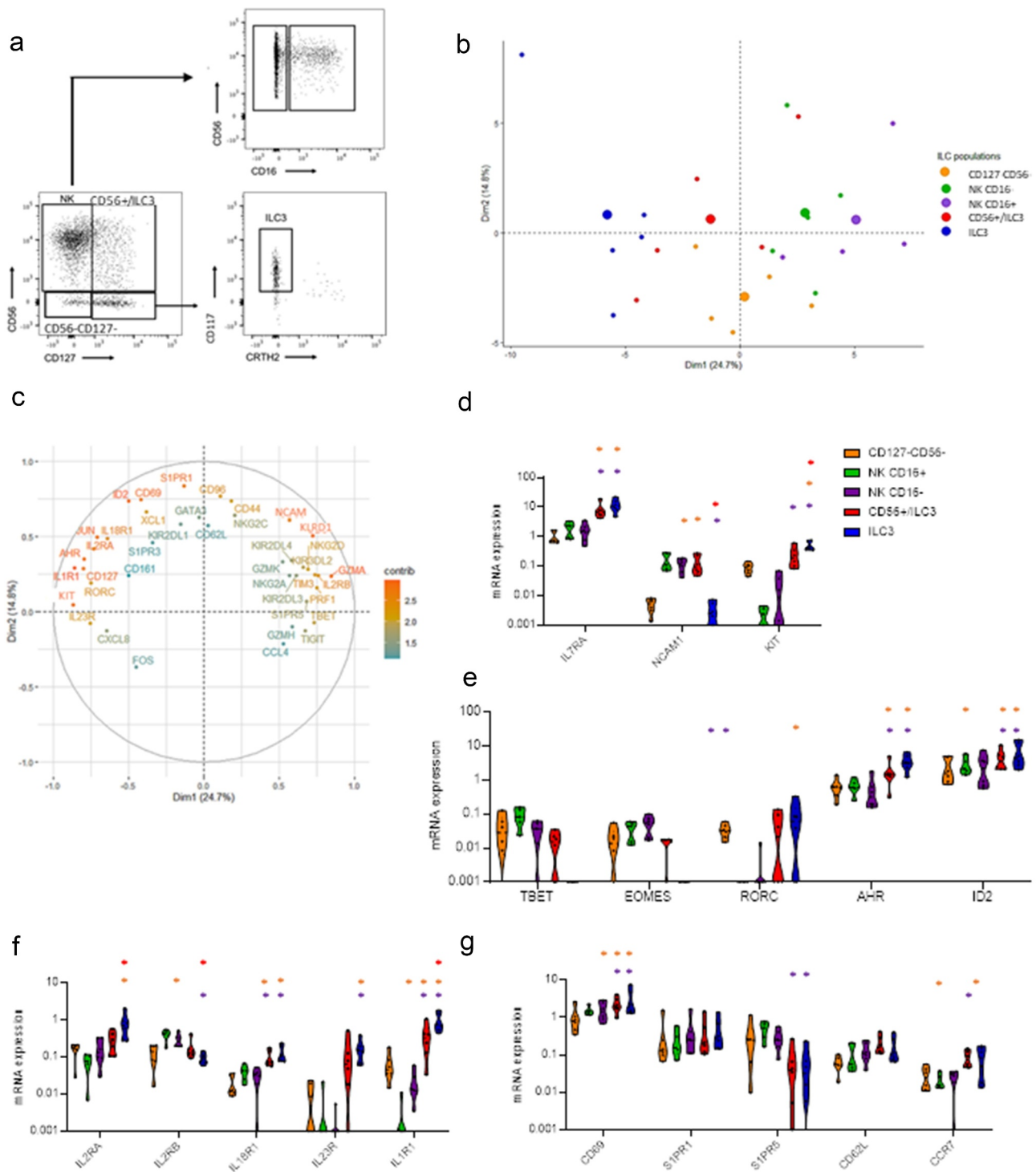


Figure 5. Transcriptomic profile of ILC from TD-LN. Gating strategy used to sort ILC subsets (a). Principal component analysis (PCA) of ILC subsets sorted from TD-LN ($n = 4/5$) (b). Graph of PCA variables, colored according to the contribution of each variable (c). mRNA expression levels for the principal variables contributing to PC1 and PC2, including definition markers for the ILC subsets, transcription factors, cytokine receptors, and markers of migration. A Wilcoxon's matched-pairs test was used to compare expression levels between two populations ($* p < .05$) (d-g).

h-ILC3s. CD127⁻CD56⁻ cells and NK cells expressed comparable levels of *EOMES*, *Tbet*, and *AHR*; they also expressed *GZMA/B*, *PRF1*, and *IFNG* (Figure 5(e)).

Cytokines are essential for the development and activation of ILCs. *IL2RA* and *IL2RB* genes were expressed by all the subsets, with ILC3 cells expressing more *IL2RA* and NK cells expressing more *IL2RB* (Figure 5(f)). CD127⁻CD56⁻ cells expressed low levels of IL2R genes. Cytokines such as IL18,

IL23, and IL1 β can activate ILC3 type functions. The genes coding for their receptors were highly expressed by ILC3s and CD56⁺/ILC3s, whereas their expression was low in NK cells and CD127⁻CD56⁻ cells.

We also examined the expression of the genes involved in tissue residency and migration (Figure 5(g)). *CD69* transcript was detected at high levels in NK cells and ILC3s from TD-LNs, whereas the membrane expression of the

corresponding protein was low (Figure 4(g)). All the ILC populations expressed high levels of *S1PR1* and *CD62L*, whereas *S1PR5* was mostly expressed by NK cells and *CCR7* by h-ILC.

In TD-LNs and tumors, NK cells predominated and their expansion in TD-LN was associated with a reduced representation of the CD56⁺/ILC3 population. NK cells infiltrating tumor and metastatic LNs were characterized by altered expression of activating receptors such as NKp46, NKp30. Hierarchic clustering (Fig S4) indicated that CD56⁺/ILC3s expressed specific ILC3 definition markers (Fig S4A), displayed similar cytokines and chemokines receptor (Fig S4A, C) but acquired a molecular profile related to CD16⁺ NK cells (Fig S3B). CD127⁻CD56⁻ NK cells exhibited the NK specific markers, resembled ILC3 for NK specific transcripts, and exhibited a unique profile for cytokine and chemokines receptors (Fig S4C).

Functional properties of ILCs in metastatic LN

Numerous studies indicate that tumors modulate the function of NK cells, and h-ILC are known to rapidly respond to changes in their environment. To assess the functional ILC behavior in TD-LN, we analyzed transcript levels for genes involved in cytotoxicity and immune regulation (Figure 6(a)). *PRF1*, *GZMA*, *GZMB*, and *IFN γ* transcript levels were high in NK cells, CD127⁻CD56⁻ ILC, and CD56⁺/ILC3s compared to ILC3s. For ILC3s and CD56⁺/ILC3s from TD-LN, *TNFA* transcripts were elevated and no *IL22* expression was detected. In a metastatic environment, ILC expressed higher levels of genes involved in antitumor functions (Figure 6(b)). CD56⁺/ILC3s from TD-LNs expressed high levels of *PRF1*, *GZMK*, and *TNFA*. High levels of *TNFA* were observed in ILC3s from TD-LNs.

Altogether, the transcriptomic profiles of ILCs infiltrating TD-LNs reflected the presence of ILCs that displayed molecular profiles compatible with antitumor functions.

In functional assays, NK, and CD56⁻CD127⁻ cells from TD-LN, activated overnight with IL-2+ IL-12, degranulated in response to stimulation with K562 – an HLA-I⁻ target of NK cells. Interestingly, stimulation with MCF7 – an HLA-I⁺ breast cancer cell line – did not induce degranulation (Figure 6(c)). The low spontaneous (no target) and K562-induced degranulation of IL-2+ IL-12-activated CD56⁺/ILC3s and ILC3s were not significantly different, indicating that NKR engagement was not involved in K562 lysis. Cytokine activation of ILC3 subsets induced a modest degranulation not significantly increased by K562. When activated by cytokines, NK cells and to a lesser extend CD127⁻CD56⁻ cells responded to K562 stimulation.

IL-2+ IL-12-activated NK cells produced IFN γ following K562 stimulation (Figure 6(c)). Percentages of IFN γ ⁺ CD56⁺/ILC3s activated by IL-2+ IL-12 were low varied among samples and did not increase in response to K562. ILC3s did not produce IFN γ , as expected based on the undetectable level of *IFNG* transcripts. Activated NK cell subsets and CD56⁺/ILC3s, produced TNF α in response to both K562 and MCF7 stimulation (Figure 6(d)). ILC3s expressing high levels of *TNFA* transcripts (Figure 6(a)) also produced TNF α in response to K562 and MCF7 (Figure 6(d)). There was no significant correlation between clinico-biological data in a series of patients.

Discussion

The aim of this report was to characterize the ILC populations infiltrating LN and to investigate the impact of BC tumor on the plasticity of the ILC populations in metastatic TD-LN. Specific mAbs and molecular probe panels to concomitantly assess the cytotoxic and helper ILCs were validated in HD-LN. The tools were then used to analyze ILC from metastatic TD-LN in BC patients.

First, phenotypic analyses identified 4 ILC subsets – NK cells including CD16⁻ and CD16⁺ subsets, ILC3s, and a prominent CD56⁺/ILC3s subset that account for 40% of the total HD-LN ILCs. Molecular analyses were performed by multiplex qPCR on 100 sorted cells from each ILC subset, as single-cell analyses did not generate detectable signals for most genes, despite pre-amplification. Furthermore, qPCR values obtained on non-activated ILC subsets were low, highlighting the difficulties linked to handling resting ILC, and imposing attention when considering the results. However, PCA analyses outlined distinct gene profiles in the ILC subsets, extending their phenotyping characterization. The major h-ILC subset, CD56⁺/ILC3s, from HD-LN expressed the genes coding for the TF ROR γ t and AHR involved in the ILC3 maturation, and T-bet and Eomes required for NK cell maturation. CD56⁺/ILC3s also expressed the genes coding for the cytotoxic molecules perforin and granzymes, and low IFN γ transcript levels. They shared with the ILC3s, transcripts for GM-CSF, IL-22, IL1R1, and ILR23. Unlike the ILC3 cells, CD56⁺/ILC3s acquire NK cell behavior in response to cytokine activation. Cytotoxic CD127⁺CD94⁺ ILC3s were described in human tonsils that were unable to differentiate into NK cells with IL-15, produced IL-22 and remained RORC⁺.⁴³ In tonsils, CD127⁺RORC⁺ cells, precursors of CD56⁺CD127⁺RORC⁺ NKp46⁺ were distinct from the NK cell lineage and demonstrated some NK functionality – such as the production of IFN γ and TNF α , and moderate cytotoxicity.⁴⁴ Unlike the NK cells that respond to IL-15, the NKp46⁺CD127⁺ROR γ t⁺ cells produce IFN γ in response to IL-2 and IL-12 stimulation.^{45,46} CD56⁺ILC3 from mesenteric HD-LN may correspond to ILC/NK precursors that give rise to NK cells and ILC3.⁴⁷ Part of the CD56⁺/ILC3s from LN, expressing CD94 (and KLRD1 transcripts), may correspond to cytotoxic ILC3s. High expression of AHR and IL1R1 in CD56⁺ILC3 may prevent the differentiation of stage 3 CD34⁻CD117⁺CD94⁻ NK cells into mature NK cells producing IFN γ and cytotoxic molecules¹¹ in homeostatic condition.

Invasion of the LN by tumor cells modifies the microenvironment.⁴⁸ Invasion by tumor cells particularly affects the composition of ILC subsets of TD-LN and impacts on the phenotype and activation status of NK cells, ILC3s and CD56⁺/ILC3s. Comparison between donor's and patient's LNs (Fig. S5) shows high percentages of NCR⁻ NK cells in TD-LN, while NCR⁺ NK cells, CD56⁺ILC3 and CD69⁺ILC3 are decreased compared to HD-LN. The tumor challenge may favor CD56⁺ILC3 differentiation into NK-like cells. Lytic CD56⁺ ILC1-like cells were described in blood and tissues.⁴⁹ CD56⁺/ILC3s from TD-LN that express *PRF1*, *GZMA*, degranule, and release cytokine indicating their anti-tumor functions; however, killing assay should be performed to ascertain whether these ILCs from HD-LN and TD-LN differently kill

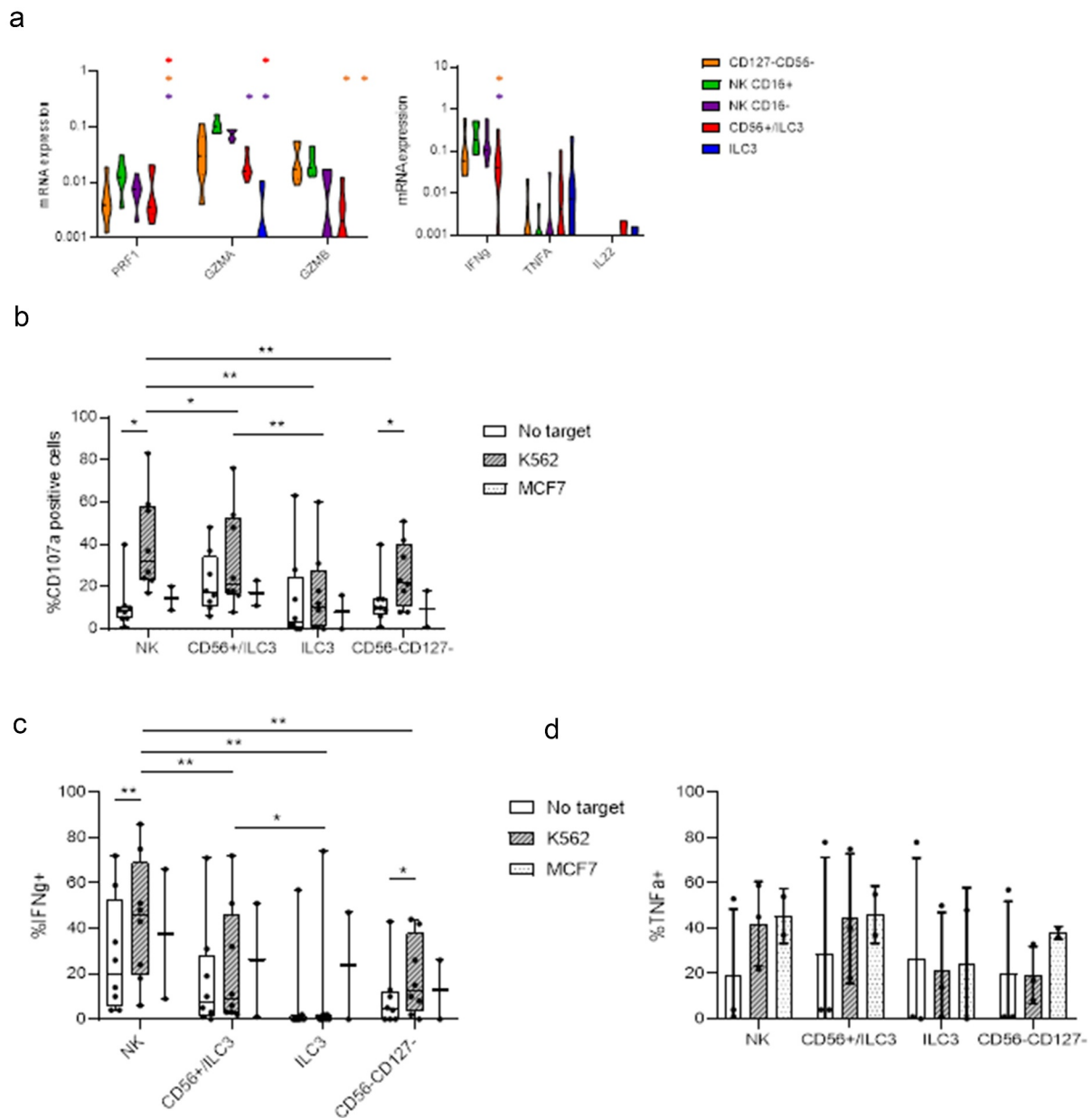


Figure 6. Functions of ILC from TD-LN. mRNA expression levels for cytotoxic molecules and cytokines in TD-LN ILC subsets ($n = 5/8$) (a). ILC were activated overnight with IL-2+ IL-12 and stimulated for 6 h with K562 or MCF7. Then, percentages of degranulating cells (CD107a-positive cells; $n = 8$) (b) and cells producing intracellular IFN γ ($n = 8$) (c) or TNF α ($n = 3$) (d) were determined by flow cytometry; 'no target' corresponds to spontaneous response (B, C, D). A Wilcoxon's matched-pairs test was used to compare expression levels between two populations (* $p < .05$, ** $p < .01$) (c-f).

tumor cells. Murine RORC⁺ ILC suppress tumor growth following IL-12 activation, and acquire an NK-like phenotype with up-regulation of NK cell functions.^{50,51} TD-LN-derived CD56⁺/ILC3s and ILC3s display high expression of TNF α and reduced of IL-22 expression. ILC3 production of TNF α , not that of IL-22 or GM-CSF can be induced by lung tumor cell lines following NKp44 stimulation.^{21,52}

Although NK cells are involved in the control of metastasis formation,⁵³ the tumor microenvironment alters NK cells. Tumor infiltrating and blood NK cells from BC patients display decreased levels of activating receptors and are non-cytotoxic.⁵⁴⁻⁵⁶ In a murine BC model, the transferred NK cells that arrived at the tumor showed reduced NKp46 expression compared to NK cells infiltrating the spleen, and NCR expression

was restored by IL-12 and anti-TGF mAbs.⁵⁷ The presence of NCR⁺ NK cells infiltrating BC tumors and TD-LNs, despite high transcript expression, suggests that tumor-derived factors such as TGF and prostaglandins PGE2/Cox2 may alter NK cell proteome profiles. The presence of NKG2A^{high} NK cells in TD-LNs likely reduces their cytotoxic functions.⁵⁸ However, NK from TD-LN exhibit an activated molecular profile, high levels of NCR, NKG2D, DNAM-1, PRF1, Granzymes, and IL2RB, IL18R transcripts, and most NK subsets (except CD127⁻CD56⁻ NKs) respond to IL-2+ IL12 activation. Thus, cytokines may cause the cells to reverse their local anergic profile. It is of note that IL-15 may further favor expansion/activation of NK cells and maintain metastatic BC cells dormancy.^{58,59}

In BC patients, the proinflammatory cytokine TNF α , which is known to promote tumor growth, enhances migration of and tissue invasion by tumor cells, and contributes to chemotherapy resistance.⁶⁰ Anti-TNF α therapies are being evaluated for treatment of BC, and blockade of ILC3 could synergize with these therapies. Recently, dysfunctional ILC3s driving colorectal cancer progression and causing immunotherapy resistance were characterized.⁶¹

Migration of ILCs may be affected in tumors and TD-LNs. NK cells are known to traffic from the tissues to the LN in a CD62L-, CCR7-dependent manner.^{62,63} In TD-LNs decreased numbers of CD69⁺ resident ILCs were observed, with only a few cells expressing this marker, even though the corresponding gene – *CD69* – was expressed at high levels by TD-LN ILCs. The CD69 membrane expression, which requires S1PR1 function, controls the retention of lymphocytes in LNs.⁶⁴ Although *S1PR1* was expressed at similar levels in HD-LN and TD-LN, it may be post-transcriptionally regulated. In TD-LNs, the membrane expression of CD69 might be prevented by S1PR1, thus allowing circulation of ILCs.⁶⁵ Circulating ILCs between the tumor and the TD-LNs may induce the redistribution and plasticity of the ILCs in TD-LNs. The NKp46⁺CD69⁻ NK cells in TD-LNs may correspond to cells migrating from tumor to the draining LNs. Alternatively, such altered ILCs may have been induced locally when the metastatic tumor cells invaded the TD-LNs. Although it cannot be excluded that LN ILC differ according to the anatomical site, however, the similarities between ILC from tumor and TD-LN samples favor the impact of the tumor microenvironment on ILCs.

Current immunotherapies have been developed mostly to restore T cells at the tumor site. Emerging strategies to stimulate immune activation in LNs are interesting approaches for the next generation of cancer therapies. In mice, TD-LNs are essential in the response to PD1/PDL1 blockade therapy.⁶⁶ Moreover, the loco-regional administration of ICB, targeting delivery to the TD-LNs, enhances the efficacy of treatment.⁶⁷ In LNs, ILCs are localized at the T-B interface where they can interact with T cells, possibly influencing their responses to immunotherapies. NK cells from TD-LN express lower surface-levels of NCRs, but nevertheless, they present an activated transcriptomic profile, suggesting that the right signal could restore activation. We previously showed that IL-15 activated TD-LN NK cells efficiently killed BC cell lines.⁵⁸

NK-based immunotherapies should therefore be considered in combination with other immunotherapies. In contrast, our results suggest that the ILC3 activation might induce a pro-tumor immune response, with TNF α production. Similarly, ROR γ ⁺ILC3s were shown to correlate with LN metastases in BC.⁶⁸ Based on these observations, blockade of ILC3 activity should also be considered in combination with current therapies.

Acknowledgments

We thank the platform of Institut de Recherche Saint-Louis for its support with molecular and FACS analyses. The authors thank Maude Delost for project management.

Disclosure statement

No potential conflict of interest was reported by the author(s).

Funding

EP, and CS received funds from Agence Nationale de la Recherche (ANR) ANR-10-IDEX-0001-02 PSL⁺ and ANR-11-LABX-0043; CIC IGR-Curie 1428 (Center for Clinical Investigation) and INCADGOSInserm_10.13039/501100006364 Institut National Du Cancer 12554.

ORCID

Anne Caignard  <http://orcid.org/0000-0001-9923-6045>

Author contributions

LR designed and performed the experiments, analyzed the data, and wrote the manuscript. MB and VB were implicated in the validation of the tools and methodology to assess ILC. FR provided the LN from organ donors. JD and CS prepared the samples from BC patients. EP, AT, ND, EP, and CS discussed and contributed to writing the manuscript. AC designed and conducted the project and wrote the manuscript. AV-S, EB provided the biological material from cancer patients.

Ethics approval and consent to participate

TDLNs and tumors were collected from breast cancer patients having undergone standard-of-care surgical resection at the Institut Curie Hospital (Paris, France), in accordance with institutional ethical guidelines and informed consent was obtained. The protocol was approved by the Ethical Committee of Curie Institut (“Comité de la Recherche Institutionnel,” CRI-0804- 2015). LN from organ donors were obtained in compliance with the institutional regulations of the Agence de Biomedecine (Paris). All authors have read the manuscript and consent to its publication.

References

- Hazenber MD, Spits H. Human innate lymphoid cells. *Blood*. 2014;124(5):700–709. doi:10.1182/blood-2013-11-427781.
- Yudanin NA, Schmitz F, Flamar AL, Thome JJC, Tait Wojno E, Moeller JB, Schirmer M, Latorre IJ, Xavier RJ, Farber DL, et al. Spatial and temporal mapping of human innate lymphoid cells reveals elements of tissue specificity. *Immunity*. 2019;50(2):505–519 e504. doi:10.1016/j.immuni.2019.01.012.
- Koh J, Kim HY, Lee Y, Park IK, Kang CH, Kim YT, Kim J-E, Choi M, Lee -W-W, Jeon YK, et al. IL23-Producing human lung cancer cells promote tumor growth via conversion of innate lymphoid cell 1 (ILC1) into ILC3. *Clin Cancer Res*. 2019;25(13):4026–4037. doi:10.1158/1078-0432.CCR-18-3458.
- Pfefferle A, Jacobs B, Haroun-Izquierdo A, Kveberg L, Sohlberg E, Malmberg KJ. Deciphering natural killer cell homeostasis. *Front Immunol*. 2020;11:812.
- Raykova A, Carrega P, Lehmann FM, Ivanek R, Landtwing V, Quast I, Lünemann JD, Finke D, Ferlazzo G, Chijioko O, et al. Interleukins 12 and 15 induce cytotoxicity and early NK-cell differentiation in type 3 innate lymphoid cells. *Blood Adv*. 2017;1(27):2679–2691. doi:10.1182/bloodadvances.2017008839.
- Simoni Y, Fehlings M, Kloverpris HN, McGovern N, Koo SL, Loh CY, Lim S, Kurioka A, Fergusson JR, Tang C-L, et al. Human innate lymphoid cell subsets possess tissue-type based heterogeneity in phenotype and frequency. *Immunity*. 2018;48(5):1060. doi:10.1016/j.immuni.2018.04.028.

7. Crinier A, Dumas PY, Escaliere B, Piperoglou C, Gil L, Villacreces A, Vély F, Ivanovic Z, Milpied P, Narni-Mancinelli É, et al. Single-cell profiling reveals the trajectories of natural killer cell differentiation in bone marrow and a stress signature induced by acute myeloid leukemia. *Cell Mol Immunol*. 2021;18(5):1290–1304. doi:10.1038/s41423-020-00574-8.
8. Crinier A, Kerdiles Y, Vienne M, Cozar B, Vivier E, Berruyer C. Multidimensional molecular controls defining NK/ILC1 identity in cancers. *Semin Immunol*. 2020;101424:1–11.
9. Crinier A, Vivier E, Blery M. Helper-like innate lymphoid cells and cancer immunotherapy. *Semin Immunol*. 2019;41:101274. doi:10.1016/j.smim.2019.04.002.
10. Hughes T, Becknell B, Freud AG, McClory S, Briercheck E, Yu J, Mao C, Giovenzana C, Nuovo G, Wei L, et al. Interleukin-1beta selectively expands and sustains interleukin-22+ immature human natural killer cells in secondary lymphoid tissue. *Immunity*. 2010;32(6):803–814. doi:10.1016/j.immuni.2010.06.007.
11. Hughes T, Becknell B, McClory S, Briercheck E, Freud AG, Zhang X, Mao H, Nuovo G, Yu J, Caligiuri MA, et al. Stage 3 immature human natural killer cells found in secondary lymphoid tissue constitutively and selectively express the TH 17 cytokine interleukin-22. *Blood*. 2009;113(17):4008–4010. doi:10.1182/blood-2008-12-192443.
12. Freud AG, Yu J, Caligiuri MA. Human natural killer cell development in secondary lymphoid tissues. *Semin Immunol*. 2014;26(2):132–137. doi:10.1016/j.smim.2014.02.008.
13. To B, Isaac D, Andrechek ER. Studying lymphatic metastasis in breast cancer: current models, strategies, and clinical perspectives. *J Mammary Gland Biol Neoplasia*. 2020;25(3):191–203. doi:10.1007/s10911-020-09460-5.
14. Fehniger TA, Cooper MA, Nuovo GJ, Cella M, Facchetti F, Colonna M, Caligiuri MA. CD56bright natural killer cells are present in human lymph nodes and are activated by T cell-derived IL-2: a potential new link between adaptive and innate immunity. *Blood*. 2003;101(8):3052–3057. doi:10.1182/blood-2002-09-2876.
15. Mackley EC, Houston S, Marriott CL, Halford EE, Lucas B, Cerovic V, Filbey KJ, Maizels RM, Hepworth MR, Sonnenberg GF, et al. CCR7-dependent trafficking of RORgamma(+) ILCs creates a unique microenvironment within mucosal draining lymph nodes. *Nat Commun*. 2015;6(1):5862. doi:10.1038/ncomms6862.
16. Carrega P, Bonaccorsi I, Di Carlo E, Morandi B, Paul P, Rizzello V, Cipollone G, Navarra G, Mingari MC, Moretta L, et al. CD56 bright perforin low noncytotoxic human NK cells are abundant in both healthy and neoplastic solid tissues and recirculate to secondary lymphoid organs via afferent lymph. *J Immunol*. 2014;192(8):3805–3815. doi:10.4049/jimmunol.1301889.
17. Shi FD, Ljunggren HG, La Cava A, Van Kaer L. Organ-specific features of natural killer cells. *Nat Rev Immunol*. 2011;11(10):658–671. doi:10.1038/nri3065.
18. Lanier LL. Natural killer cell receptor signaling. *Curr Opin Immunol*. 2003;15(3):308–314. doi:10.1016/S0952-7915(03)00039-6.
19. Moretta L, Moretta A. Unravelling natural killer cell function: triggering and inhibitory human NK receptors. *EMBO J*. 2004;23(2):255–259. doi:10.1038/sj.emboj.7600019.
20. Moretta A, Bottino C, Vitale M, Pende D, Cantoni C, Mingari M, Biassoni R, Moretta L. Activating receptors and coreceptors involved in human natural killer cell-mediated cytotoxicity. *Annu Rev Immunol*. 2001;19(1):197–223. doi:10.1146/annurev.immunol.19.1.197.
21. Glatzer T, Killig M, Meisig J, Ommert I, Luetke-Eversloh M, Babic M, Paclik D, Blüthgen N, Seidl R, Seifarth C, et al. RORgammat(+) innate lymphoid cells acquire a proinflammatory program upon engagement of the activating receptor NKp44. *Immunity*. 2013;38(6):1223–1235. doi:10.1016/j.immuni.2013.05.013.
22. Hoorweg K, Peters CP, Cornelissen F, Aparicio-Domingo P, Papazian N, Kazemier G, Mjösberg JM, Spits H, Cupedo T. Functional Differences between Human NKp44- and NKp44+ RORC+ Innate Lymphoid Cells. *Front Immunol*. 2012;3:72. doi:10.3389/fimmu.2012.00072.
23. Raulat DH. Roles of the NKG2D immunoreceptor and its ligands. *Nat Rev Immunol*. 2003;3(10):781–790. doi:10.1038/nri1199.
24. Gilfillan S, Chan CJ, Cella M, Haynes NM, Rapaport AS, Boles KS, Andrews DM, Smyth MJ, Colonna M. DNAM-1 promotes activation of cytotoxic lymphocytes by nonprofessional antigen-presenting cells and tumors. *J Exp Med*. 2008;205(13):2965–2973. doi:10.1084/jem.20081752.
25. Natarajan K, Dimasi N, Wang J, Mariuzza RA, Margulies DH. Structure and function of natural killer cell receptors: multiple molecular solutions to self, nonself discrimination. *Annu Rev Immunol*. 2002;20(1):853–885. doi:10.1146/annurev.immunol.20.100301.064812.
26. Chan CJ, Martinet L, Gilfillan S, Souza-Fonseca-Guimaraes F, Chow MT, Town L, Ritchie DS, Colonna M, Andrews DM, Smyth MJ, et al. The receptors CD96 and CD226 oppose each other in the regulation of natural killer cell functions. *Nat Immunol*. 2014;15(5):431–438. doi:10.1038/ni.2850.
27. de Andrade LF, Smyth MJ, Martinet L. DNAM-1 control of natural killer cells functions through nectin and nectin-like proteins. *Immunol Cell Biol*. 2014;92(3):237–244. doi:10.1038/icb.2013.95.
28. Glasner A, Levi A, Enk J, Isaacson B, Viukov S, Orlanski S, Scope A, Neuman T, Enk CD, Hanna JH, et al. NKp46 receptor-mediated interferon-gamma production by natural killer cells increases fibronectin 1 to alter tumor architecture and control metastasis. *Immunity*. 2018;48(2):396–398. doi:10.1016/j.immuni.2018.01.010.
29. Guillerey C, Huntington ND, Smyth MJ. Targeting natural killer cells in cancer immunotherapy. *Nat Immunol*. 2016;17(9):1025–1036. doi:10.1038/ni.3518.
30. Lopez-Soto A, Bravo-San Pedro JM, Kroemer G, Galluzzi L, Gonzalez S. Involvement of autophagy in NK cell development and function. *Autophagy*. 2017;13(3):633–636. doi:10.1080/15548627.2016.1274486.
31. van der Weyden L, Arends MJ, Campbell AD, Bald T, Wardle-Jones H, Griggs N, Velasco-Herrera MDC, Tüting T, Sansom OJ, Karp NA, et al. Genome-wide in vivo screen identifies novel host regulators of metastatic colonization. *Nature*. 2017;541(7636):233–236. doi:10.1038/nature20792.
32. Arianfar E, Shahgordi S, Memarian A. Natural killer cell defects in breast cancer: a Key pathway for tumor evasion. *Int Rev Immunol*. 2021;40(3):197–216. doi:10.1080/08830185.2020.1845670.
33. Ferretti E, Carlomagno S, Pesce S, Muccio L, Obino V, Greppi M, Solari A, Setti C, Marcenaro E, Della Chiesa M, et al. Role of the main non HLA-specific activating NK receptors in pancreatic, colorectal and gastric tumors surveillance. *Cancers*. 2020;12(12):3705–3725.
34. Heinze A, Grebe B, Bremm M, Huenecke S, Munir TA, Graafen L, Frueh JT, Merker M, Rettinger E, Soerensen J, et al. The Synergistic Use of IL-15 and IL-21 for the Generation of NK Cells From CD3/CD19-Depleted Grafts Improves Their ex vivo Expansion and Cytotoxic Potential Against Neuroblastoma: perspective for Optimized Immunotherapy Post Haploidentical Stem Cell Transplantation. *Front Immunol*. 2019;10:2816. doi:10.3389/fimmu.2019.02816.
35. Dahlberg CI, Sarhan D, Chrobok M, Duru AD, Alici E. Natural killer cell-based therapies targeting cancer: possible strategies to gain and sustain anti-tumor activity. *Front Immunol*. 2015;6:605. doi:10.3389/fimmu.2015.00605.
36. Ma X, Holt D, Kundu N, Reader J, Goloubeva O, Take Y, Fulton AM. A prostaglandin E (PGE) receptor EP4 antagonist protects natural killer cells from PGE2-mediated immunosuppression and inhibits breast cancer metastasis. *Oncoimmunology*. 2013;2(1):e22647. doi:10.4161/onci.22647.
37. Salimi M, Wang R, Yao X, Li X, Wang X, Hu Y, Chang X, Fan P, Dong T, Ogg G, et al. Activated innate lymphoid cell populations accumulate in human tumour tissues. *BMC Cancer*. 2018;18(1):341. doi:10.1186/s12885-018-4262-4.

38. Kotecha N, Krutzik PO, Irish JM. Web-based analysis and publication of flow cytometry experiments. *Curr Protoc Cytometry Chapter*. 2010;10:Unit10.17.
39. Lim AI, Li Y, Lopez-Lastra S, Stadhouders R, Paul F, Casrouge A, Serafini N, Puel A, Bustamante J, Surace L, et al. Systemic human ILC precursors provide a substrate for tissue ILC differentiation. *Cell*. 2017;168(6):1086–1100. doi:10.1016/j.cell.2017.02.021.
40. Bar-Ephraim YE, Cornelissen F, Papazian N, Konijn T, Hoogenboezem RM, Sanders MA, Westerman BA, Gönültas M, Kwekkeboom J, Den Haan JMM, et al. Cross-Tissue transcriptomic analysis of human secondary Lymphoid organ-residing ILC3s reveals a quiescent state in the absence of inflammation. *Cell Rep*. 2017;21(3):823–833. doi:10.1016/j.celrep.2017.09.070.
41. Fuchs A, Vermi W, Lee JS, Lonardi S, Gilfillan S, Newberry RD, Cella M, Colonna M. Intraepithelial type 1 innate lymphoid cells are a unique subset of IL-12- and IL-15-responsive IFN-gamma-producing cells. *Immunity*. 2013;38(4):769–781. doi:10.1016/j.immuni.2013.02.010.
42. Simoni Y, Fehlings M, Kloverpris HN, McGovern N, Koo SL, Loh CY, Lim S, Kurioka A, Fergusson JR, Tang CL, et al. Human innate Lymphoid cell subsets possess tissue-type based heterogeneity in phenotype and frequency. *Immunity*. 2017;46:148–161.
43. Krabbendam L, Heesters BA, Kradolfer CMA, Spits H, Bernink JH. Identification of human cytotoxic ILC3s. *Eur J Immunol*. 2021;51(4):811–823. doi:10.1002/eji.202048696.
44. Crellin NK, Trifari S, Kaplan CD, Cupedo T, Spits H. Human NKp44+IL-22+ cells and LTi-like cells constitute a stable RORC+ lineage distinct from conventional natural killer cells. *J Exp Med*. 2010;207(2):281–290. doi:10.1084/jem.20091509.
45. Bernink JH, Peters CP, Munneke M, te Velde AA, Meijer SL, Weijer K, Hreggvidsdottir HS, Heinsbroek SE, Legrand N, Buskens CJ, et al. Human type 1 innate lymphoid cells accumulate in inflamed mucosal tissues. *Nat Immunol*. 2013;14(3):221–229. doi:10.1038/ni.2534.
46. Cella M, Otero K, Colonna M. Expansion of human NK-22 cells with IL-7, IL-2, and IL-1 β reveals intrinsic functional plasticity. *Proc Natl Acad Sci U S A*. 2010;107(24):10961–10966. doi:10.1073/pnas.1005641107.
47. Chen L, Youssef Y, Robinson C, Ernst GF, Carson MY, Young KA, Scoville SD, Zhang X, Harris R, Sekhri P, et al. CD56 expression marks human group 2 innate lymphoid cell divergence from a shared NK cell and group 3 innate lymphoid cell developmental pathway. *Immunity*. 2018;49:464–476. doi:10.1016/j.immuni.2018.02.017.
48. Sleeman JP. The lymph node pre-metastatic niche. *J Mol Med*. 2015;93(11):1173–1184. doi:10.1007/s00109-015-1351-6.
49. Salome B, Gomez-Cadena A, Loyon R, Suffiotti M, Salvestrini V, Wyss T, Vanoni G, Ruan DF, Rossi M, Tozzo A, et al. CD56 as a marker of an ILC1-like population with NK cell properties that is functionally impaired in AML. *Blood Adv*. 2019;3(22):3674–3687. doi:10.1182/bloodadvances.2018030478.
50. Nussbaum K, Burkhard SH, Ohs I, Mair F, Klose CSN, Arnold SJ, Diefenbach A, Tugues S, Becher B. Tissue microenvironment dictates the fate and tumor-suppressive function of type 3 ILCs. *J Exp Med*. 2017;214(8):2331–2347. doi:10.1084/jem.20162031.
51. Vonarbourg C, Mortha A, Bui VL, Hernandez PP, Kiss EA, Hoyler T, Flach M, Bengsch B, Thimme R, Hölscher C, et al. Regulated expression of nuclear receptor ROR γ confers distinct functional fates to NK cell receptor-expressing ROR γ innate lymphocytes. *Immunity*. 2010;33(5):736–751. doi:10.1016/j.immuni.2010.10.017.
52. Carrega P, Loiacono F, Di Carlo E, Scaramuccia A, Mora M, Conte R, Benelli R, Spaggiari GM, Cantoni C, Campana S, et al. NCR(+) ILC3 concentrate in human lung cancer and associate with intratumoral lymphoid structures. *Nat Commun*. 2015;6(1):8280. doi:10.1038/ncomms9280.
53. Lopez-Soto A, Gonzalez S, Smyth MJ, Galluzzi L. Control of Metastasis by NK Cells. *Cancer Cell*. 2017;32(2):135–154. doi:10.1016/j.ccell.2017.06.009.
54. Mamessier E, Pradel LC, Thibult ML, Drevet C, Zouine A, Jacquemier J, Houvenaeghel G, Bertucci F, Birnbaum D, Olive D, et al. Peripheral blood NK cells from breast cancer patients are tumor-induced composite subsets. *J Immunol*. 2013;190(5):2424–2436. doi:10.4049/jimmunol.1200140.
55. Mamessier E, Sylvain A, Bertucci F, Castellano R, Finetti P, Houvenaeghel G, Charaffe-Jaufret E, Birnbaum D, Moretta A, Olive D, et al. Human breast tumor cells induce self-tolerance mechanisms to avoid NKG2D-mediated and DNAM-mediated NK cell recognition. *Cancer Res*. 2011;71:6621–6632.
56. Mamessier E, Sylvain A, Thibult ML, Houvenaeghel G, Jacquemier J, Castellano R, Gonçalves A, André P, Romagné F, Thibault G, et al. Human breast cancer cells enhance self tolerance by promoting evasion from NK cell antitumor immunity. *J Clin Invest*. 2011;121(9):3609–3622. doi:10.1172/JCI45816.
57. Krneta T, Gillgrass A, Chew M, Ashkar AA. The breast tumor microenvironment alters the phenotype and function of natural killer cells. *Cell Mol Immunol*. 2016;13(5):628–639. doi:10.1038/cmi.2015.42.
58. Frazao A, Messaoudene M, Nunez N, Dulphy N, Roussin F, Sedlik C, Zitvogel L, Eliane Piaggio E, Toubert A, Caignard A. CD16(+)NKG2A(high) natural killer cells infiltrate breast cancer-draining lymph nodes. *Cancer Immunol Res*. 2019;7:208–218.
59. Correia AL, Guimaraes JC, Auf der Maur P, De Silva D, Trefny MP, Okamoto R, Bruno S, Schmidt A, Mertz K, Volkmann K, et al. Hepatic stellate cells suppress NK cell-sustained breast cancer dormancy. *Nature*. 2021;594:566–571.
60. Cruceriu D, Baldasici O, Balacescu O, Berindan-Neagoe I. The dual role of tumor necrosis factor-alpha (TNF-alpha) in breast cancer: molecular insights and therapeutic approaches. *Cell Oncol*. 2020;43(1):1–18. doi:10.1007/s13402-019-00489-1.
61. Goc J, Lv M, Bessman NJ, Flamar AL, Sahota S, Suzuki H, Teng F, Putzel GG, Eberl G, Withers DR, et al. Dysregulation of ILC3s unleashes progression and immunotherapy resistance in colon cancer. *Cell*. 2021;184(19):5015–5030. doi:10.1016/j.cell.2021.07.029.
62. Castellarin M, Watanabe K, June CH, Kloss CC, Posey AD Jr. Driving cars to the clinic for solid tumors. *Gene Ther*. 2018;25(3):165–175. doi:10.1038/s41434-018-0007-x.
63. Castriconi R, Carrega P, Dondero A, Bellora F, Casu B, Regis S, Ferlazzo G, Bottino C. Molecular mechanisms directing migration and retention of natural killer cells in human tissues. *Front Immunol*. 2018;9:2324. doi:10.3389/fimmu.2018.02324.
64. Cyster JG, Schwab SR. Sphingosine-1-phosphate and lymphocyte egress from lymphoid organs. *Annu Rev Immunol*. 2012;30(1):69–94. doi:10.1146/annurev-immunol-020711-075011.
65. Shiow LR, Rosen DB, Brdiczka N, Xu Y, An J, Lanier LL, Cyster JG, Matloubian M. CD69 acts downstream of interferon-alpha/beta to inhibit S1P1 and lymphocyte egress from lymphoid organs. *Nature*. 2006;440(7083):540–544. doi:10.1038/nature04606.
66. Fransen MF, Schoonderwoerd M, Knopf P, Camps MG, Hawinkels LJ, Kneilling M, van Hall T, Ossendorp F. Tumor-draining lymph nodes are pivotal in PD-1/PD-L1 checkpoint therapy. *JCI Insight*. 2018;2(23):e124507.
67. Francis DM, Manspeaker MP, Schudel A, Sestito LF, O'Melia MJ, Kissick HT, Pollack BP, Edmund EK, Waller EK, Thomas, SN. Blockade of immune checkpoints in lymph nodes through locoregional delivery augments cancer immunotherapy. *Sci Transl Med*. 2020;12.
68. Irshad S, Flores-Borja F, Lawler K, Monypenny J, Evans R, Male V, et al. ROR γ Innate lymphoid cells promote lymph node metastasis of breast cancers. *Cancer Res*. 2017;77(5):1083–1096. doi:10.1158/0008-5472.CAN-16-0598.